ELSEVIER

Chemical Geology 162 (1999) 15–31

CHEMICAL GEOLOGY
INCLUDING
ISOTOPE GEOSCIENCE

www.elsevier.com/locate/chemgeo

Precipitation of Fe(III) oxyhydroxide deposits from shallow-water hydrothermal fluids in Tutum Bay, Ambitle Island, Papua New Guinea

Thomas Pichler [a,*,1], Jan Veizer [a,b]

[a] *Ottawa-Carleton Geoscience Centre, University of Ottawa, Department of Geology, P.O. Box 450, Stn. A, Ottawa, ON, Canada K1N 6N5*
[b] *Institut für Geologie, Ruhr Universität, 44780 Bochum, Germany*

Received 12 October 1998; accepted 15 April 1999

Abstract

Previous research on sea floor Fe(III) oxyhydroxide deposits has focused primarily on deep-sea, hydrothermal systems found along volcanically active portions of the mid-ocean ridges and on hydrogenetic deposits formed in deep basins and along continental shelves. There is, however, not much known about their formation in shallow-water settings associated with volcanic islands. The hydrothermal system at Ambitle Island, Papua New Guinea provides an excellent opportunity to study the formation of Fe(III) oxyhydroxides in a shallow-water setting. Precipitation from the hydrothermal solution is caused by mixing with seawater. Based on a $^{87}Sr/^{86}Sr$ mixing model, the calculated minimum and maximum seawater fractions are approximately 11 and 57%, respectively. Thus, precipitation of Tutum Bay Fe(III) oxyhydroxides takes place at a temperature range between approximately 60 and 93°C. The chemical composition shows low Mn contents ($Fe/Mn > 600$), and elements that are usually enriched in Fe(III) oxyhydroxides, such as Co and V are below crustal abundance and well below their concentrations in island-arc volcanics. Arsenic concentrations, on the other hand, are by two orders of magnitude higher than those in other marine deposits. Rare earth element (REE) concentrations reflect their concentration in the hydrothermal fluids rather than seawater. The crystallinity of the deposits increases with age, as protoferrihydrite is apparently altered to Fe-smectite and hematite, and As-bearing minerals are formed. Contact with seawater, and therefore oxidizing conditions, seems to be the factor increasing the crystallinity.

Keywords: Fe(III) oxyhydroxide; Hydrothermal system; Shallow water; Arsenic; Papua New Guinea

1. Introduction

Massive sulfides, Mn-oxyhydroxides, Fe(III) oxyhydroxides and Fe-smectites are the principal seafloor deposits associated with hydrothermal activity. Except for a few intra-plate locations, massive sulfides are usually associated with deep-water, high-temperature hydrothermal systems along mid-ocean ridges and in deep back-arc basins. Fe(III) oxyhydroxides, on the other hand, are apparently the prominent intra-plate deposits that form in shallow water, low temperature hydrothermal systems in seamount and island-arc environments (Malahoff et al., 1982; Var-

* Corresponding author. Tel.: +1-813-974-2236; fax: +1-813-974-2654; e-mail: pichler@chuma.cas.usf.edu

[1] New address: Department of Geology, University of South Florida, 4202 E. Fowler Ave., Tampa, FL 33615, USA.

0009-2541/99/$ - see front matter
PII: S0009-2541(99)00068-6

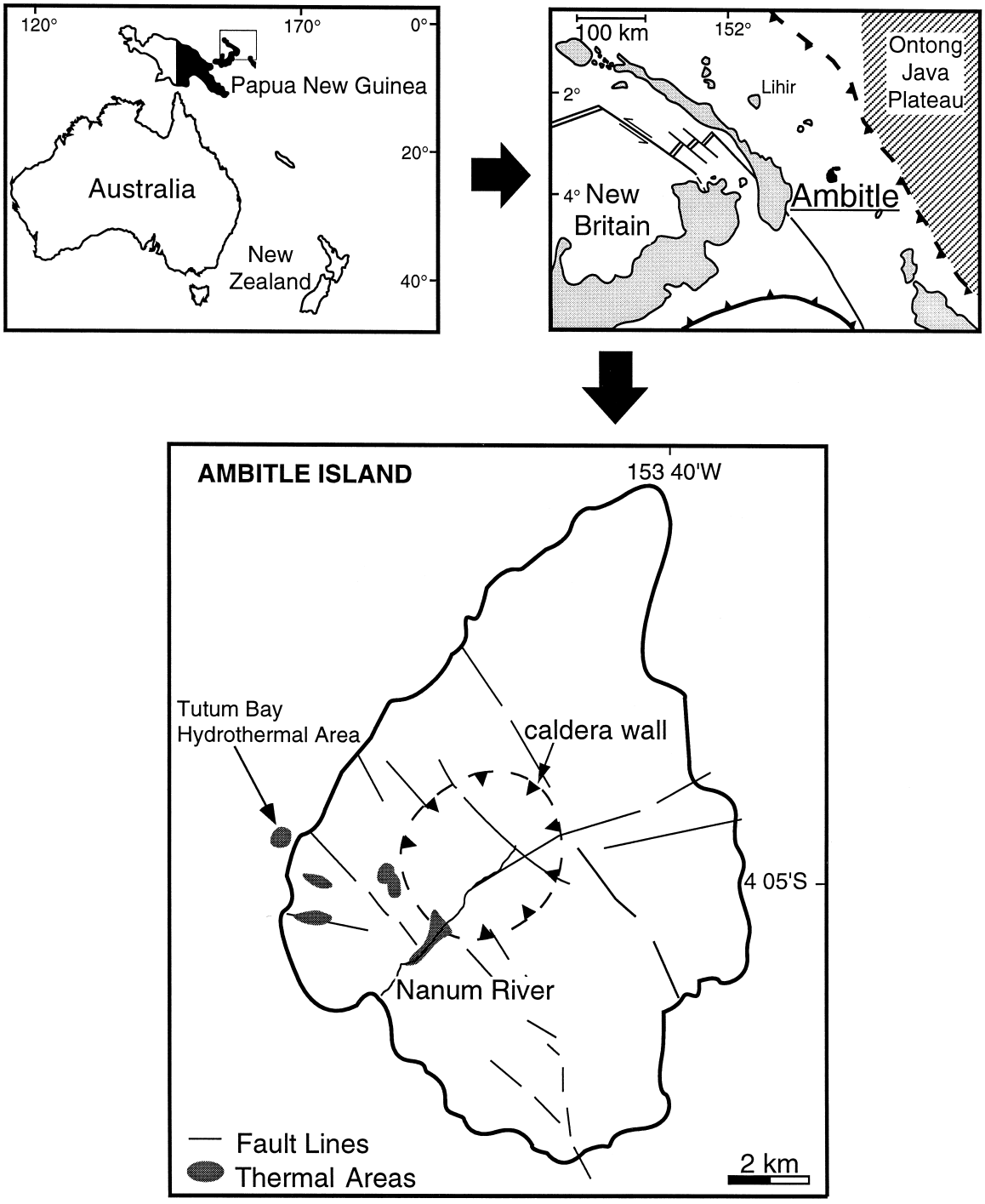

Fig. 1. Location of Ambitle Island, one of the Feni islands in eastern Papua New Guinea (modified after Licence et al., 1987 and Pichler and Dix, 1996). Geothermal areas indicated in dark are primarily along the western side of the island.

navas and Cronan, 1991; Michard et al., 1993). Several models have been proposed to explain their formation and the absence of sulfide is one of the main factors that would promote the precipitation of a hydroxide phase at the expense of a sulfide mineral (e.g., Seyfried and Bischoff, 1977; Edmond et al., 1979; Rona, 1984; Puteanus et al., 1991; Stoffers et al., 1993). All models agree that mixing with seawater is the final step that causes precipitation and that the sulfide is removed from the hydrothermal fluid via precipitation of metal sulfides in the sub-seafloor. However, they differ to some degree in explaining metal sulfide precipitation. Processes that are considered include adiabatic boiling (e.g., Stoffers et al., 1993), H_2S exsolution (e.g., Puteanus et al., 1991) and mixing with seawater in the sub-seafloor (e.g., Sedwick et al., 1992).

The most common precipitates are hematite, goethite, lepidocrocite, ferrihydrite and protoferrihydrite, and their preferential formation depends on physicochemical conditions (Murray, 1979). For brevity, these minerals are referred to collectively as Fe(III) oxyhydroxides. Natural occurrences of Fe(III) oxyhydroxides, other than those associated with submarine hydrothermal activity, include gossans, ironstones, soils, hot springs, and stream beds (e.g., Chao and Theobald, 1976; Murray, 1979). Many Fe(III) oxyhydroxide deposits are of economic interest, either directly for mining or for geochemical prospecting. The ochers, ironstones and gossans on the island of Cyprus, for example, were among the first ores to be mined commercially, dating back to pre-Roman times (Weisgerber, 1982). Hydrous iron oxides are significant indicator minerals in geochemical exploration because they effectively scavenge important ore metals from the weathering zone (e.g., Chao and Theobald, 1976). Fe(III) oxyhydroxides are particularly important constituents in marine sediments in volcanically-active coastal areas where they can effect the composition of local seawater and therefore marine life (Pichler et al., 1999a). The mainly amorphous nature of these deposits makes

Table 1
Description of Tutum Bay hydrothermal Fe(III) oxyhydroxide precipitates

Sample	Location	Description	XRD scans
FV-1A	Vent 1	massive layers with alternating colors ranging from dark brown to dark orange; indurated and relatively hard compared to the other Fe-oxyhydroxides	protoferrihydrite, gypsum, hematite, As_2O_4, As_2O_5, Fe-smectite
FV-1B	Vent 1	softer layer of dark orange color from beneath FV-1A	n.d.
V-1B	Vent 1	Fe-precipitate on a volcanic boulder	protoferrihydrite
V-2B I	Vent 2	massive layer of reddish brown relatively hard Fe-oxyhydroxide that precipitated on dead coral fragments and aragonite	protoferrihydrite, Fe-smectite, claudetite (As_2O_3)
V-2B II	Vent 2	soft layer of yellow brown color from beneath V-2B I	protoferrihydrite
V-2B III	Vent 2	very thin intermediate layer between V-2B I and V-2B II; may contain significant amounts of both V-2B I and V-2B II	
V-4.1D	Vent 4	Fe-oxyhydroxide coating volcanic fragments and fragments of dead corals, contains some aragonite	protoferrihydrite
V-2 (97) I	Vent 4	very thin hard dark greenish brown layer on a coral skeleton that fell partly over the vent orifice; contains significant amounts of V-2 (97) II, was in contact with mainly seawater at the time of sampling; collected from the side of the coral opposite to the vent	protoferrihydrite, Fe-smectite
V-2 (97) II	Vent 4	very soft orange to orange brown layer on a coral skeleton that fell partly over the vent orifice; collected from the side of the coral that faced the vent	protoferrihydrite

n.d. = not determined.

them efficient scavengers and, as a result, they are thought to be the most important removal mechanism from seawater for many trace elements, including the rare earth elements (e.g., Fleet, 1984).

2. Description of study area and Fe(III) oxyhydroxide deposits

The study area lies along the southwest margin of Ambitle Island, one of the Feni islands in the southernmost island group of the Tabar-Feni island-arc (Fig. 1). The island is part of a Quaternary stratovolcano with a central eroded caldera built on poorly exposed Oligocene marine limestone (Wallace et al., 1983). Volcanic strata (interbedded lava flows, lahar deposits, tuffs, and scoriae) dip radially from the island, presumably extending beneath the shelf. Several geothermal areas are located primarily along the western coast and in the western part of the caldera near breaches in the caldera wall (Fig. 1). Hot mud pools, springs of chloride and acid sulfate waters, and a few low temperature fumaroles are present, with temperature and pH values ranging from 67 to 100°C and 1.9 to 9.1, respectively (Wallace et al., 1983).

Submarine hydrothermal venting occurs at Tutum Bay (Fig. 1) in shallow (5–10 m) water along the inner shelf that contains a patchy distribution of coral–algal reefs surrounded by medium to coarse-grained mixed carbonate-volcaniclastic sand and gravel (Pichler and Dix, 1996). Two types of venting are observed. (1) Focused discharge of a clear, hydrothermal fluid that occurs at discrete ports, 10–15 cm in diameter. Fluid temperatures at vent orifices are between 89 and 98°C. (2) Dispersed or diffuse discharge consisting of streams of gas bubbles emerging directly through the sandy to pebbly unconsolidated sediment and through fractures in volcanic rocks.

Fe(III) oxyhydroxides are present throughout Tutum Bay where they form thin coatings on sediment grains in areas of high seafloor temperature. Massive layers and extensive filling of sediment pore space, however, are restricted to the vicinity of vent sites. Here they coat volcanic boulders in bright orange, form distinct bands on corals skeletons, aragonite and Fe-calcite and/or precipitate as massive layers in open spaces. They can vary in color from a bright orange to very dark brown (almost black) and in hardness from <1 (talc) to about 2.5 (between gypsum and calcite). A complete listing of all Fe(III) oxyhydroxide samples collected, is given in Table 1.

Samples V-2-97 and V-2 were collected from the same vent, except that V-2-97 was taken approximately 18 months later. Sample V-2-97 provides us with the opportunity to estimate the rate of precipitation and to investigate the very early stages of Fe(III) oxyhydroxide precipitation. In February 1997 an unusually strong storm struck Ambitle Island from the southwest (Philip Tolain, 1997, personal communication) and heavy seas caused extensive damage to coral reefs and shoreline. In Tutum Bay several large coral heads were tipped over and several colonies of branching corals were destroyed. During that process, part of a Staghorn coral must have fallen over the main orifice of vent 2. At the time of sampling, those branches exposed to the hydrothermal fluid were coated with very soft and fragile orange to orange brown Fe(III) oxyhydroxide deposits approximately 5–7 mm thick. Given the period between the onset of deposition and sampling, precipitation rates could be as high as 1 cm/year. Precipitation on coral branches continues to roughly 20 cm above the orifice, but deposits gradually become thinner with distance. Those sides of the deposits that were distal to the vent fluid and, therefore, more exposed to seawater than hydrothermal fluid had a very thin greenish brown hard surface layer (V-2-97 II). Beneath that layer, however, the material was identical to the Fe(III) oxyhydroxides exposed mainly to the hydrothermal fluid.

3. Analytical procedures

Bulk Fe(III) oxyhydroxide material was separated from its substrate, rinsed with deionized water to remove halite and carefully crushed in an agate mortar. Sample powders were dried at room temperature to prevent goethite to hematite conversion (Deer et al., 1992). Hand specimens, polished thin and thick sections were examined using standard transmitted and reflected light microscopy. Mineral iden-

tification was confirmed by scanning electron microscope (SEM), transmission electron microscope (TEM), Mössbauer spectroscopy and powder and single-crystal X-ray diffractometry (XRD). Small sample chips were carbon coated and mounted on aluminum stubs for SEM analysis on a Cambridge Stereoscan 360 instrument, fully integrated with an Oxford Instruments (Link) eXL-II energy dispersive

Table 2
Major, minor, trace element and Sr-isotope composition of Tutum Bay hydrothermal Fe(III) oxyhydroxide precipitates

Sample	Unit	FV-1A	FV-1B	V-1B	V-2B I	V-2B II	V-2B III	V-4.1D
SiO_2	%	20.90	14.50	14.10	13.30	12.30	17.20	14.80
TiO_2	%	< 0.02	< 0.02	< 0.02	< 0.02	< 0.02	< 0.02	0.12
Al_2O_3	%	< 0.2	< 0.2	< 0.2	< 0.2	< 0.2	< 0.2	1.04
$Fe_2O_3^T$	%	44.70	52.50	50.90	52.70	54.10	50.80	44.40
MnO	%	0.09	0.08	0.11	0.07	0.07	0.07	0.08
MgO	%	0.83	0.73	1.07	0.78	0.82	1.07	1.28
CaO	%	2.57	1.70	2.51	1.82	1.96	1.63	7.09
Na_2O	%	0.69	0.48	0.67	0.82	1.09	0.76	0.96
K_2O	%	0.20	0.15	0.17	0.12	0.14	0.16	0.33
P_2O_5	%	0.21	0.22	0.19	0.22	0.25	0.20	0.26
CO_2^T	%	0.2	0.2	2.1	1.5	1.6	1.3	7.1
LOI	%	22.4	21.9	18.3	18.3	18.7	19.6	19.2
S^T	%	0.05	0.03	< 0.02	0.02	0.04	< 0.02	< 0.02
Total	%	93.1	91.8	89.8	89.8	90.9	93.2	96.2
Ag	ppm	0.2	0.1	1.5	0.4	0.3	0.4	5.6
Au	ppb	< 17	< 17	< 41	< 40	< 41	< 40	< 40
As	ppm	55 000	49 000	57 000	60 000	62 000	54 000	49 000
Ba	ppm	180	220	80	110	130	100	70
Be	ppm	35	50	42	39	34	38	28
Br	ppm	< 5	11	< 4	< 5	< 4	< 5	< 4
Co	ppm	< 5	< 5	< 5	< 5	< 5	< 5	< 5
Cr	ppm	24	30	28	16	26	31	45
Cs	ppm	5.3	3.5	1	1.1	0.98	1.9	3.2
Cu	ppm	33	41	14	15	15	13	160
Ga	ppm	2.1	1	0.9	0.8	0.9	0.9	3.1
Hf	ppm	< 0.05	0.06	< 0.05	< 0.05	< 0.05	< 0.05	0.17
Hg	ppm	< 5	< 1	< 5	< 5	< 5	< 5	< 5
In	ppm	< 0.05	< 0.05	0.08	0.08	0.06	0.08	0.06
Mo	ppm	3.6	1.7	0.8	0.8	0.7	0.8	1.3
Nb	ppm	< 10	< 10	< 10	< 10	< 10	< 10	18
Ni	ppm	0.08	0.29	0.25	0.18	0.23	0.2	0.55
Pb	ppm	16	35	14	15	16	15	49
Rb	ppm	13	7.1	3.9	3.8	3.9	5.5	9.7
Sb	ppm	240	260	170	180	160	190	190
Se	ppm	< 6	< 3	< 6	< 11	< 6	< 11	< 6
Sr	ppm	1100	770	910	940	940	780	1500
Tl	ppm	4.2	3.1	0.82	2	1.9	1.9	0.59
U	ppm	0.92	0.63	0.73	0.34	0.58	0.47	0.88
V	ppm	< 5	< 5	14	< 5	6	< 5	80
W	ppm	< 12	< 7	< 10	< 10	< 11	< 11	< 10
Y	ppm	10	18	21	9.3	8.1	9.1	20
Zn	ppm	33	56	40	29	24	32	49
Zr	ppm	1	3.2	1.1	1	1	1	6.6
$^{87}Sr/^{86}Sr$		0.70458	n.d.	0.70701	0.70512	0.70478	0.70489	0.70604

n.d. = not determined; Maximum error for $^{87}Sr/^{86}Sr$ values is ± 0.000009 2 standard errors.

X-ray (EDX) microanalyzer. XRD analyses were performed on a Philips PW 3710, stepping 0.02° 2θ from 2.00° to 88.00° 2θ using copper X-radiation generated at 45 kV and 40 mA.

The chemical composition of the Fe(III) oxyhydroxides were determined by micro-beam analyses on carbon-coated polished thin sections and bulk chemical methods on powdered sample material. Proton microprobe analyses were carried out on the Ruhr University, Bochum micro-PIXE, on spots of approximately 5 μm diameter, using a 3 MeV beam (Bruhn et al., 1995) and elemental concentrations were calculated with the GUPIX software package (Maxwell et al., 1995).

Trace element concentrations in Tutum Bay Fe(III) oxyhydroxide deposits were generally low and, therefore, below the detection limit of conventional microbeam methods. In order to obtain more detailed information on the chemical composition of the hydrothermal Fe(III) oxyhydroxides, bulk analyses was carried out on selected samples (Table 2). For these samples major elements were obtained by X-ray fluorescence (XRF). As, Au, Br, Hg, Sb, Se and W were determined by neutron activation analyses (NAA). Ag, Cd, Cs, Hf, In, Mo, Nb, Pb, Rb, Ta, Tl, U, Y, Zr and rare earth elements (REEs) were determined by inductively coupled plasma mass spectrometry (ICP-MS) and Ba, Be, Co, Cr, Cu, Ni, Sc, Sr, and V were determined by inductively coupled plasma emission spectrometry (ICP-ES). XRF and ICP analyses were carried out at the Geological Survey of Canada and NAA was performed by Activation Labs in Ancaster, Ontario. Analytical errors are as follows: $<2\%$ for XRD, $<5\%$ for ICP-ES (except $<10\%$ for Ag, Ba and Sr), $<10\%$ for ICP-MS and ~ 15–20% for NAA.

4. Results

Hardness and color of the Fe(III) oxyhydroxides are related to each other such that the darker the color the harder the precipitate. Based on sample hardness, color, general appearance and stratigraphic position, the relative age of Tutum Bay Fe(III) oxyhydroxide deposits was assigned qualitatively from oldest to youngest in the order FV-1, V-2, V-1B, V-4.1 and V-2-97.

4.1. Mineralogy

A combination of XRD and SEM/EDX analyses was applied to clarify the mineralogical history and composition of the Fe(III) oxyhydroxide deposits (Table 1; Figs. 2 and 3). The X-ray amorphous nature of many Fe(III) oxyhydroxide deposits reflects their very fine grain size and colloidal origin (e.g., Puteanus et al., 1991). Indeed, Mössbauer spectroscopy confirmed the amorphous nature for Tutum Bay Fe(III) oxyhydroxides and particle sizes of less than 100 Å. The two diffractograms in Fig. 2 represent the two mineralogical endmembers of Tutum Bay deposits. Sample V-2-97 has no distinct peaks, except for two broad humps at approximately 38 and 62° 2θ ($d = 2.5$ Å and 1.5 Å). These two humps may be groups of adjacent, diffuse reflections and

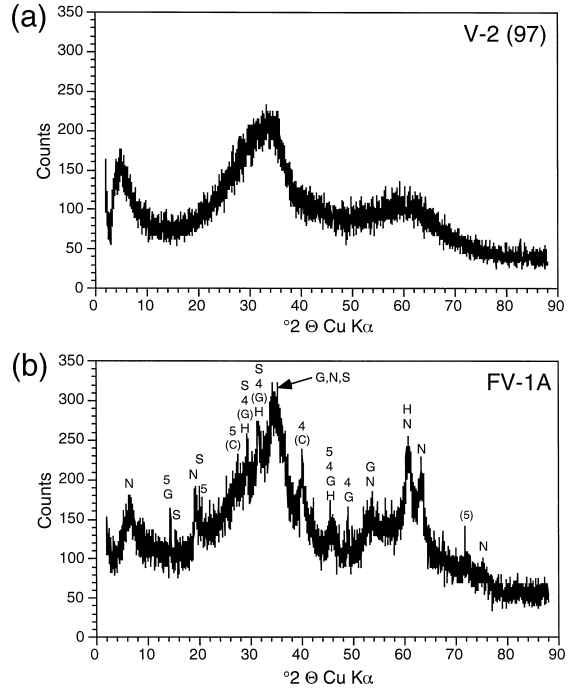

Fig. 2. Diffractometer patterns for sample V-2 (97) II (a) and FV-1A (b). The two patterns clearly demonstrate the increasing crystallinity with increasing age. V-2 (97) contains only protoferrihydrite, whereas in FV-1A several sharp peaks are superimposed on top of the typical protoferrihydrite pattern: N: smectite (nontronite), G: gypsum, C: claudetite, S: scorodite, H: hematite, 4: As_2O_4 and 5: As_2O_5. Letters in brackets indicate doubtful assignment of peaks to minerals.

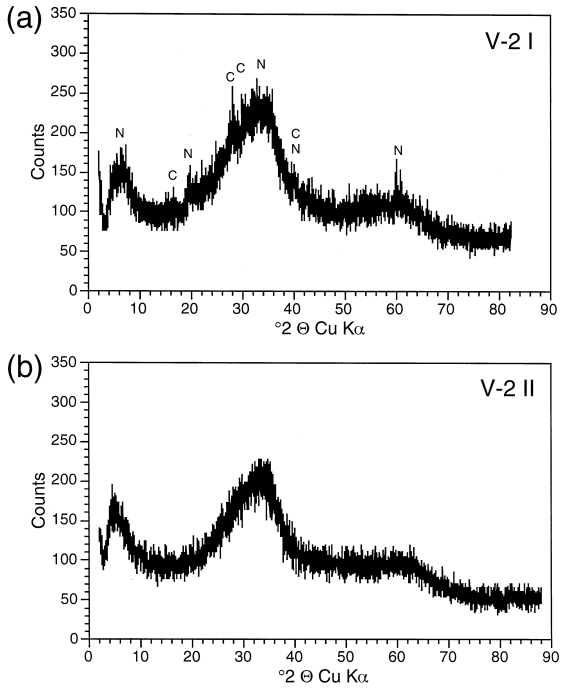

Fig. 3. Diffractometer patterns for sample V-2 I (a) and V-2 II (b). The two patterns demonstrate the importance of seawater contact during aging. V-2 I although slightly younger than V-2 II already contains two crystalline minerals, because it remained in contact with either seawater or a mixture of seawater and vent fluid (seawater ≫ vent fluid). C: claudetite, N: smectite (nontronite).

indicate the presence of hydrous iron oxide (Giessen, 1966; Towe and Bradley, 1967). Chukhrov et al. (1973) proposed the name protoferrihydrite for hydrous iron oxides that give only two reflections (2.5 and 1.5 Å) and ferrihydrite for those that give five reflections (2.52, 2.25, 1.97, 1.72 and 1.48 Å). They also concluded that the lesser amount of reflections for protoferrihydrite indicates the beginning stage of crystallization.

Sample FV-1A also shows the two broad humps at approximately 38 and 62° 2θ, but several other sharp peaks are clearly observable (Fig. 2b). Mineral identification was aided by SEM/EDX analyses and showed As_2O_5, scorodite ($FeAsO_4 \cdot 2H_2O$), gypsum and Fe-smectite. As_2O_4 and hematite are likely present, but could not be unequivocally confirmed because they share X-ray reflections with As_2O_5, gypsum and Fe-smectite (Fig. 2b). It was not possible to determine the exact variety of Fe-smectite, but circumstantial evidence indicates nontronite, a dioctahedral Fe-smectite. The appearance and greenish color of sample V-2-97 I (Table 1) is identical to that of a nontronite-rich Fe(III) oxyhydroxide deposit in the Woodlark Basin (see Fig. 6 in Binns et al., 1993). Nontronite has been found to be the dominant smectite in other Fe(III) oxyhydroxide deposits in submarine settings (e.g., Alt, 1988; Stoffers et al., 1990; Puteanus et al., 1991; Hekinian et al., 1993) where the presence of oxygenated seawater either prevents the formation of Fe-rich saponite (Fe^{2+}-smectite) or causes the transformation from saponite to nontronite (Andrews, 1980). Kankite ($FeAsO_4 \cdot 3.5H_2O$), hydrogenarsenate ($H_5As_3O_{10}$) and/or hydrated hydrogenarsenate ($H_3As_4O_4 \cdot 3H_2O$) may also occur in the Tutum Bay deposits, but could not be confirmed unambiguously by XRD or SEM/EDX.

The outer layer of sample V-2B (V-2B I, Table 1 and Fig. 3a) represents a mineralogical composition intermediate between the two samples in Fig. 2 (V-2-97 and FV-1A). Here the presence of Fe-smectite and claudetite (As_2O_3) could be confirmed. The reflections are not as strong as those in sample FV-1A, indicating either a lesser amount of mineral present or poorer crystallinity. Reflections for Fe-smectite and claudetite are absent in the softer, less dark material of sample V-2 II that was collected from beneath V-2 I. This scan is almost identical to that of sample V-2-97.

In addition to the two broad humps at 38° and 62° 2θ ($d = 2.5$ Å and 1.5 Å), a somewhat sharper reflection was observed at approximately 4.2° 2θ ($d \sim 20$ Å) in samples V-2-97 and V-2 II (Figs. 2a and 3b). This reflection is partly an artifact that arises from the small-particle diffraction tail of two-line ferrihydrite that is cut off by the instrumental shape function (D. Rancourt, personal communication). This peak seems to broaden and shift to the right with increasing crystallinity of the Fe(III) oxyhydroxide, indicating the formation of Fe-smectite (Fig. 3a).

4.2. Chemistry

Tutum Bay Fe(III) oxyhydroxide deposits show approximately the same chemical composition, with the exception of Fe, Si, Ca, CO_2^T, and Sr in sample

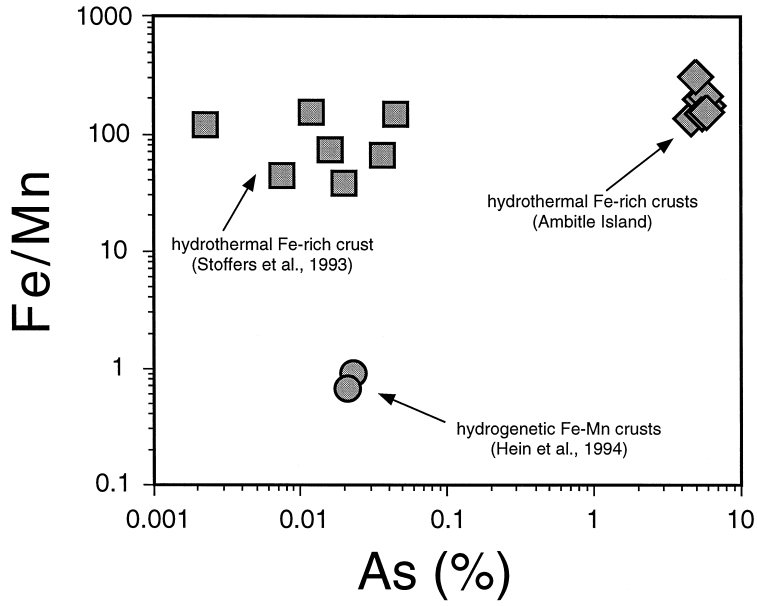

Fig. 4. Scatter plot of As concentration vs. Fe/Mn ratio on a log scale. Tutum Bay Fe(III) oxyhydroxide deposits have similar Fe/Mn ratios as hydrothermal Fe-rich crusts from south Pacific seamounts, but As values are more than two orders of magnitude higher.

4.1D (Table 2). The relatively elevated contents of Ca, CO_2^T and Sr in 4.1D are in good agreement with the assumption that this sample is slightly contaminated with aragonite. Fe and Si are negatively correlated ($r = 0.81$ and $n = 7$), Fe and Ca are negatively correlated ($r = 0.84$ and $n = 7$) and Ca and CO_2^T are positively correlated ($r = 0.94$ and $n = 7$). This indicates that some of the variation in chemical composition can be explained by simple contamination with minor amounts of aragonite. Mössbauer spectroscopic analyses of samples FV-1 and V-2 confirmed that iron is exclusively present in its trivalent state.

Manganese (Fe/Mn > 600) and combined Co, Ni and Cu contents are very low in Tutum Bay Fe(III) oxyhydroxides which places them into the lower left corner of the diagnostic ternary diagram of Bonatti et

Table 3
Proton probe traverse across Tutum Bay Fe(III) oxyhydroxide sample FV-1A

Point	1	2	3	4	5	6	7	8	9
color	orange brown	orange	orange brown	dark brown	dark brown	brown	orange brown	dark brown	brown
Fe	380 000	330 000	420 000	370 000	407 000	420 000	410 000	390 000	430 000
As	59 000	54 000	55 000	76 000	64 000	65 000	57 000	71 000	61 000
Zn	57	73	76	78	73	70	68	88	63
Sr	350	390	350	1000	700	490	380	700	300
Sb	200	160	220	240	260	290	260	150	220
Ta	160	< 30	< 30	190	170	140	130	170	150
Ni	< 24	< 24	< 24	105	< 24	< 24	< 24	< 24	< 24
Cu	< 17	< 17	< 17	73	< 17	72	< 17	< 17	80
Y	< 6	< 6	20	< 6	< 6	< 6	< 6	< 6	20

All analyses in parts per million (ppm).

al. (1972), indicating a hydrothermal origin. Elements that are usually enriched in Fe(III) oxyhydroxides, such as Co and V (e.g., Chao and Theobald, 1976), are below crustal abundance and well below their concentration in island-arc volcanic rocks. Arsenic, on the other hand, is very high and clearly sets Tutum Bay Fe(III) oxyhydroxides apart from other submarine Fe-rich deposits (Fig. 4). Arsenic contents are as high as 6.2% if analyzed by neutron activation (Table 2) and 7.6% if analyzed by proton probe (Table 3); this difference reflecting bulk analysis in the case of NAA and unhomogenised samples in the case of proton probe. The proton probe analyses listed in Table 3 are a traverse across differently colored layers in sample FV-1A and darker layers generally have higher As concentrations. There is no correlation between Fe and As contents ($r = 0.03$, $n = 9$) and other elements are correlated as follows: As and Sr $r = 0.81$ ($n = 9$), As and Ta = 0.65 ($n = 7$), and Fe and Sr $r = 0.9$ ($n = 9$).

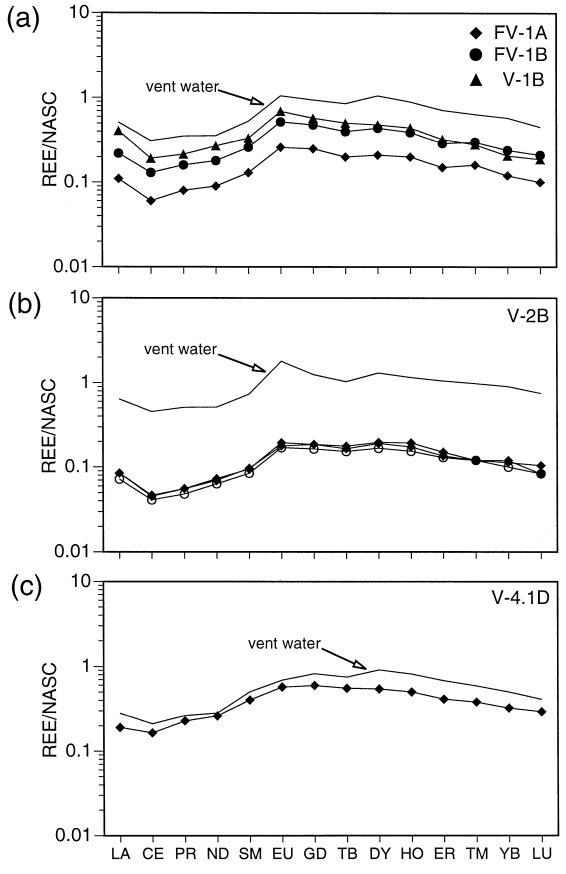

Fig. 5. North American Shale Composite (NASC) (Haskin et al., 1968) normalized REE plots for hydrothermal Fe(III) oxyhydroxide precipitates from vents 1, 2 and 4. REE concentrations for vent waters are multiplied by 10^6 and the values are interpolated for Tm and extrapolated for Lu (Pichler et al., 1999b).

North American Shale Composite (NASC) normalized REE patterns of samples FV-1A, FV-1B, V1-B and V-2B show an initial drop from La to Ce followed by a rise from the Ce minimum to an Eu maximum and a constant decrease towards a Lu minimum (Fig. 5a,b). The pattern geometry approximately resembles that of the parent hydrothermal fluid, except that the Eu peaks in the Fe(III) oxyhydroxides are not as pronounced as in the hydrothermal fluid. The sample from vent 4 is different and more closely resembles the pattern of the parent hydrothermal fluid (Fig. 5c). Relative REE concentrations initially drop from La to a Ce minimum which is followed by a rise to a Eu–Gd maximum and a slight decrease towards an intermediate Lu.

5. Discussion

5.1. Formation of Tutum Bay Fe(III) oxyhydroxide deposits

Alteration of iron bearing minerals and direct precipitation from solution are the two processes that lead to the formation of Fe(III) oxyhydroxide deposits, such as goethite, lepidocrocite, hematite and ferrihydrite. The final product is dependent on an intricate interplay between bacterial activity, pH, Eh, temperature, precipitation rate and iron concentration (e.g., Alt, 1988; Binns et al., 1993; Chao and Theobald, 1976; Chukhrov et al., 1973; Fortin et al., 1993; Hekinian et al., 1993; Murray, 1979; Puteanus et al., 1991; Schwertmann and Fischer, 1973; Stoffers et al., 1993). Direct precipitation from solution occurs either via the slow hydrolysis of Fe^{3+} or due to oxidation of Fe^{2+}-bearing solutions (e.g., Murray, 1979). The former generally leads to the formation of goethite, except from solutions containing Cl^-, which precipitate akageneite (Murray, 1979). Neither mineral was observed in Tutum Bay Fe(III) oxyhydroxides indicating that hydrolysis of Fe^{3+} is not important for their formation. In Tutum Bay vent

fluids (Eh ~ −0.17 V and pH ~ 6.1; Pichler et al., 1999b) Fe^{3+} is effectively absent and as a result, precipitation must proceed via oxidation of Fe^{2+}, through mixing with cool, alkaline, oxygenated seawater (e.g., Millero et al., 1987). The resulting increase of Eh and pH and decrease in temperature are in favor of the precipitation of Fe(III) oxyhydroxide (Fig. 6a). At the same time, conditions are not oxidizing enough to cause precipitation of a Mn-rich (Fig. 6b) or As-rich (Pichler et al., 1999a) mineral, which explains their absence in young Tutum Bay Fe(III) oxyhydroxide deposits. The same process has been called upon to explain the formation of various other Fe(III) oxyhydroxide deposits in submarine settings (e.g., Alt, 1988; Puteanus et al., 1991). Under these conditions, X-ray amorphous Fe(III) oxyhydroxides is the result, because precipitation is rapid, thus preventing the formation of a crystalline phase. Chukhrov et al. (1973) noted that rapid deposition of hydrous iron oxides, produces protoferrihydrite. Maximum precipitation rates in Tutum Bay are up to three times higher than those measured for Fe(III) oxyhydroxide deposits from Loihi Seamount (Sedwick and McMurtry, 1987; Cremer, 1995) and, as a result, protoferrihydrite is the dominant Fe-bearing phase (Table 1).

Oxidation of Fe^{2+} as a mechanism of precipitation is also supported by the use of $^{87}Sr/^{86}Sr$ as a tracer of mixing between hydrothermal fluid and seawater (Fig. 7). $^{87}Sr/^{86}Sr$ ratios are a widely used tracer in mixing processes (Faure, 1986). The mass difference between the two strontium isotopes, ^{87}Sr and ^{86}Sr, is too small to cause a measurable fractionation during precipitation. Thus the $^{87}Sr/^{86}Sr$ ratio in Fe(III) oxyhydroxide can be used as a direct measure of its ratio in the parent fluid. Assuming no conductive loss or gain of heat and seawater and hydrothermal fluid to be 30°C and 100°C, respectively, the temperature of the mixture can be calculated with the mass balance equation:

$$t_M = (1 - y)\,t_{HF} + y t_{SW} \quad (1)$$

where t_M, is the temperature of the mixture, t_{HF} is the temperature of the hydrothermal fluid and t_{SW} is

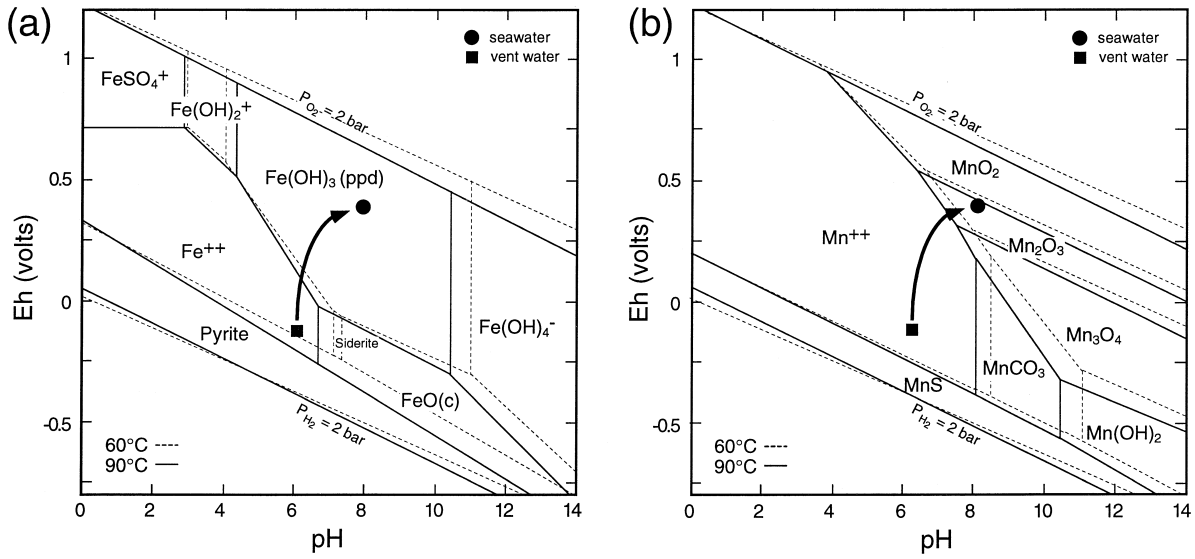

Fig. 6. (a) Calculated Eh–pH diagram for the system Fe–O–H–SO_4–HCO_3 at 60°C (dashed lines) and 90°C (solid lines) at a pressure of 2.026 bars. Thus representing the upper and lower temperature limit of Fe(III) oxyhydroxide formation. Activities for Fe^{2+}, SO_4^{2-} and HCO_3^- correspond to their respective concentration in the mixture between Tutum Bay hydrothermal fluids and seawater (Table 4) at 60° and 90°C. Thermodynamic data are from a compilation by Faure (1991). $Fe(OH)_3$ (ppd) is the field of amorphous Fe(III) oxyhydroxide. The arrow indicates the mixing trend between hydrothermal fluid and seawater. The pH is buffered due to the relatively high HCO_3^- concentration in the vent fluids. (b) The same Eh–pH diagram for the system Mn–O–H–SO_4–HCO_3. Manganese remains comparably longer in its divalent state and, therefore, in solution than Fe^{2+}, thus explaining its absence in Tutum Bay Fe(III) oxyhydroxides.

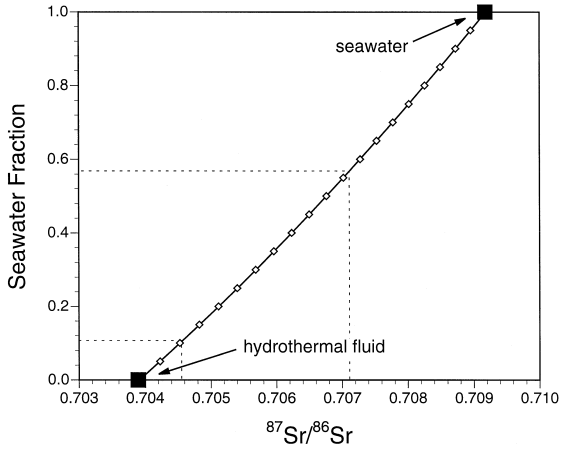

Fig. 7. Mixing curve between the hydrothermal fluid and seawater endmember (Table 4) based on $^{87}Sr/^{86}Sr$ ratios in Fe(III) oxyhydroxide precipitates. The dashed lines indicate the range of $^{87}Sr/^{86}Sr$ ratios (0.7048 to 0.7071) and the corresponding amount of seawater admixed to the hydrothermal fluid at the time of precipitation.

the temperature of seawater, and y is the seawater fraction. The calculated minimum and maximum seawater fractions are approximately 11 and 57%, respectively (Fig. 7). Thus, precipitation of Tutum Bay Fe(III) oxyhydroxides takes place within a temperature range between approximately 60° and 93°C. This model, however, cannot be used without reservation, because Fe(III) oxyhydroxide is a mixture of different minerals, and the mineral phases represent slightly different physicochemical conditions. Postdepositional absorption of Sr or exchange with seawater or hydrothermal fluid cannot be excluded due to the extreme reactivity of the Fe(III) oxyhydroxide surface (e.g., Davis and Kent, 1991). Thus, through time, Fe(III) oxyhydroxides may lose the chemical signature that represents the conditions during precipitation. Nevertheless, the temperatures that were estimated with the $^{87}Sr/^{86}Sr$ mixing model are in good agreement with precipitation temperatures reported in the literature (e.g., Chukhrov et al., 1973; Puteanus et al., 1991; Stoffers et al., 1993).

Bacteria that use the oxidation of Fe^{2+} as an energy source are often involved in the formation of Fe(III) oxyhydroxides (e.g., Chukhrov et al., 1973; Fortin et al., 1993; Leblanc et al., 1996). The active participation of bacteria in the precipitation of Tutum Bay Fe(III) oxyhydroxides could neither be confirmed nor disproved. Several rounded to subrounded Fe and Si-rich bodies, approximately 1 μm across, were observed by electron microscopy. Transmission electron microscopic (TEM) analyses, however, did not conclusively confirm the presence of bacteria, although rounded shapes were observed that could be their mineralized remnants.

The very fine grain size and colloidal origin of Fe(III) oxyhydroxide phases is reflected in their amorphous nature. However, once precipitated, aging will increase the crystallinity and generally lead to the formation of either hematite (e.g., Chukhrov et al., 1973) or goethite (e.g., Schwertmann and Fischer, 1973). Older seafloor deposits consist almost exclusively of goethite, with contents of up to 88% (Hein et al., 1994). The presence of goethite was not confirmed for Tutum Bay Fe(III) oxyhydroxide deposits (Figs. 2 and 3). The degree of crystallinity as deduced form XRD analyses, however, seems to be directly related to a) relative age of the precipitate, and b) exposure to seawater. Samples FV-1A and V-2 I, thought to be older than V-1B, V-2-97 and V-4.1D, clearly show the more complex XRD patterns. These two samples (FV-1A and V-2 I) are the outer layers of their respective Fe(III) oxyhydroxide deposits and were exposed to a mixture of seawater and hydrothermal fluid (seawater ≫ hydrothermal fluid) at the time of sampling. Samples, FV-1B and V-2 II, collected from layers just beneath FV-1A and V-2 I, were not directly exposed to seawater and contain only protoferrihydrite.

Rapid precipitation is often called upon to explain the amorphous nature of Fe(III) oxyhydroxide precipitates (e.g., Chao and Theobald, 1976; Hekinian et al., 1993). The relatively high silica concentration in Tutum Bay vent fluids may play an additional role. Freshly precipitated Fe(III) oxyhydroxide reacts strongly with silicate compounds, thus preventing further crystallization (Schwertmann, 1966; Schwertmann, 1970). Puteanus et al. (1991) suggested the formation of an X-ray amorphous nontronite resulted from rapid precipitation. Fe-smectite (assumed to be nontronite) is the first crystalline phase to form in Tutum Bay Fe(III) oxyhydroxides and its presence in the outer layer of sample V-2-97 suggests that its forms from the Fe(III) oxyhydroxide after exposure to seawater for ≤ 6 months. Nontronite is a common secondary mineral in many submarine hydrothermal

metalliferous deposits (e.g., Bischoff, 1969; McMurtry and Yeh, 1981; Murnane and Clague, 1983) and/or a product of ocean floor weathering of volcanic rocks (e.g., Stakes and Scheidegger, 1981; Rad et al., 1990; Alt, 1993; Gallahan and Duncan, 1994). Puteanus et al. (1991), who extensively reviewed the existing literature on nontronite, found that the temperature of formation, when determined by oxygen isotope thermometry was relatively low (3–57°C). Those low temperatures are in good agreement with the assumption that nontronite in Tutum Bay forms due to interaction between Fe(III) oxyhydroxide and seawater and/or a very dilute hydrothermal fluid.

We suggest that the Tutum Bay Fe(III) oxyhydroxides recrystallize and incorporate As-minerals and gypsum that were not present initially. Crystallinity increases with age, as demonstrated by samples V-2-97 and FV-1A, which are thought to represent the youngest and oldest Fe(III) oxyhydroxide deposits (Fig. 2). Recrystallization, however, commences only under oxidizing conditions and therefore, in contact with seawater, as demonstrated by sample V-2B. In this sample recrystallization was only observed in the outer layer V-2b I (Fig. 3). A detailed discussion of the formation of As-minerals been given by Pichler et al. (1999a).

5.2. The chemical composition of Tutum Bay Fe(III) oxyhydroxide deposits

In aqueous systems, scavenging of elements into and onto metal hydroxides results from: (1) coprecipitation, (2) adsorption, (3) surface complex formation, (4) ion exchange, and (5) penetration of the crystal lattice (Chao and Theobald, 1976), but it is often impossible to distinguish between coprecipitation and adsorption (Drever, 1988). Adsorption, however, has been observed to be the basis of most surface-chemical reactions (Stumm and Morgan, 1996), making it the most likely cause for the minor and trace element composition in Tutum Bay Fe(III) oxyhydroxides. Relative to arsenic, minor element concentrations are low and reflect their low concentrations in the hydrothermal fluid (Tables 2 and 4). Little information exists regarding the intensity of scavenging of elements other than the heavy metals and REEs, except that many metals that form strong OH-complexes in water also bind strongly to hydroxide surfaces (Dzombak and Morel, 1990). This is confirmed in Tutum Bay Fe(III) oxyhydroxide deposits, where trace metals that form stronger OH-complexes (e.g., Sb and Tl) are generally enriched when compared to the alkali elements K, Rb and Cs that form weaker OH-complexes. The Rb/Sb ratio, for example, is 44 in the vent fluid from vent 1 (Table 4) and only 0.023 in the corresponding Fe(III) oxyhydroxide sample (V-1B, Table 2).

The adsorption of As onto iron hydroxides is controlled by the specific surface area of the adsorbent and several experimental studies have found that adsorption onto ferrihydrite at standard conditions (temperature = 25°C and pressure = 1 bar) is generally rapid and strongest at a pH of approximately 6–7 (e.g., Pierce and Moore, 1980; Bowell, 1994; Manning and Goldberg, 1997). Comparing these experimental conditions with those present in Tutum Bay, the exceedingly high As concentrations

Table 4
Average chemical and isotopic endmember[a] compositions of Tutum Bay hydrothermal fluids for area A and area B hydrothermal fluids compared to seawater (from Pichler, 1998)

Sample	Unit	Area 1	Area 2	Seawater
pH		6.1	6.3	8.03
Cl	(ppm)	295	357	19520
Br	(ppm)	6.8	10.7	45
SO_4	(ppm)	930	880	2748
HCO_3^-	(ppm)	840	865	154
B	(ppm)	8.4	8.6	4.1
Si	(ppm)	108	105	0.2
Na	(ppm)	650	665	10450
K	(ppm)	76	94	354
Ca	(ppm)	201	180	405
Mg	(ppm)	0[a]	0[a]	1235
Li	(ppb)	1020	990	136
Mn	(ppb)	495	380	1.6
Fe	(ppb)	1720	1060	15
Rb	(ppb)	350	360	104
Sr	(ppb)	6790	6240	7990
Sb	(ppb)	8.2	9.1	0.6
Cs	(ppb)	59	63	0.5
Tl	(ppb)	4.5	5.2	0.25
As	(ppb)	820	955	3.7
$^{87}Sr/^{86}Sr$	ratio	0.70392	0.70395	0.70918
$\delta^{13}C_{VPDB}$	‰	−1.5	−1.6	1.2
$\delta^{18}O_{VSMOW}$	‰	−5.1	−5.1	0.4
δD_{VSMOW}	‰	−30.9	−30.2	6.6

[a] Endmember compositions were extrapolated assuming a zero-Mg hydrothermal fluid.

in Fe(III) oxyhydroxides are not surprising, because mixing with seawater will increase the pH of the vent fluids from initially 6 to close to 7.

The extent of mixing with seawater during precipitation, as determined by the $^{87}Sr/^{86}Sr$ mixing model, may also be imprinted in the trace element signature of Fe(III) oxyhydroxide, in particular for elements that possess a substantial concentration difference between seawater and hydrothermal fluid (Table 4). This is evident in the two samples V-1B and FV-1A that were collected at the same vent, but from different locations, and experienced therefore different mixing conditions. Sample V-1B, a thin layer coating volcanic boulders adjacent to the orifice, has a higher $^{87}Sr/^{86}Sr$ ratio (i.e., higher seawater) and lower concentrations of Cs, Rb, Sb and Tl than FV-1B, a massive layer from within the vent orifice. This corresponds with the enrichment of Cs, Rb, Sb and Tl in the vent fluids (Table 4).

Rare earth elements are known to be very effectively scavenged by Fe(III) oxyhydroxides (Koeppenkastrop and De Carlo, 1992; Koeppenkastrop et al., 1991) and as a result Tutum Bay deposits are enriched relative to the hydrothermal fluid by approximately a factor of 10^5. Unlike the hydrogenetic Fe and Mn-rich deposits, whose REE patterns are a mirror image of the seawater pattern (e.g., Fleet, 1984), at Tutum Bay the REE concentrations in Fe(III) oxyhydroxides reflect the REE concentration in the hydrothermal fluid (Pichler et al., 1999b) (Fig. 5). In seawater, REEs are undersaturated but can be removed in trace amounts by both inorganic and organic processes. The preferential uptake of light REEs in hydrogenetic Fe and Mn-rich oxyhydroxides is thought to be due to the fact that heavy REEs form stronger carbonate complexes in seawater (Lee and Bryne, 1993). The positive Ce anomaly that is generally present in hydrogenetic Fe-rich crusts, contrasts with the negative Ce anomaly in seawater and in Tutum Bay Fe(III) oxyhydroxides (Fig. 5). Goldberg (1961) proposed that Ce^{3+} in the ocean is oxidized to Ce^{4+} and precipitated as CeO_2 while the other REEs remain in their trivalent state. In addition, Ce forms colloidal ceric hydroxide (Carpenter and Grant, 1967) which may be more easily scavenged by Fe/Mn-oxyhydroxides. The negative Ce anomaly in Tutum Bay Fe(III) oxyhydroxides likely reflects the reducing nature of the vent fluids (Pichler et al., 1999b) and a high precipitation rate, which would prevent oxidation of hydrothermal Ce and the Ce uptake from seawater.

The ΣREE, although enriched by approximately 10^5 over their concentration in vent fluids (Fig. 5), is still relatively low when compared to that in hydrogenetic deposits (Fleet, 1984), but comparable to concentrations in other hydrothermal Fe(III) oxyhydroxide deposits (e.g., Stoffers et al., 1993). Olivarez and Owen (1989) found that the REE/Fe ratio in hydrothermal sediments increases with distance from the ridge axis, i.e., vent site, and argued that REE uptake from seawater is the cause. According to their ideas, low REE/Fe ratios would indicate rapid precipitation, thus preventing adsorption of seawater derived REE, whereas high REE/Fe ratios indicate a low precipitation rate, i.e., extended contact with seawater (cf. Stoffers et al., 1993). The high precipitation rates and low REE/Fe ratios observed in Tutum Bay are in general accord with this proposition, but it has to be noted that this model is only valid for a restricted time period. Its validity may be compromised if Fe(III) oxyhydroxides start to recrystallize due to extended contact with seawater, as proposed for the Tutum Bay deposits. The formation of secondary minerals, such as, hematite, goethite and Fe-smectite is accompanied by a decreases in adsorption capacity and, as a result, REEs are released. This is also suggested by the lower ΣREE in the most crystalline sample, FV-1A, when compared to samples FV-1B and V-1B (Fig. 5). While the observed REE concentrations in samples FV-1A, FV-1B and V-1B are in good agreement with theoretical considerations, it has to be noted that the change in concentration may be due to temporal physicochemical changes in the hydrothermal system.

6. A short note about mineral exploration

Anomalous arsenic concentrations have been linked to more than 20 economically important elements (Boyle and Jonasson, 1973), including the precious metals, Au, Ag and Pt. The definite role of arsenic in the ore forming process is unclear (Parker and Nicholson, 1990), nevertheless the work of Berger and Silberman (1985) and Silberman and

Berger (1985) clearly documents its utility as a tracer in delineating areas of epithermal gold mineralization. Island arcs, such as the Tabar-Feni arc, are favorable environments for the formation of epithermal ore deposits (e.g., Sillitoe, 1988; Müller and Groves, 1993; Pichler and Hutchinson, 1993). Identification of anomalous chemical signatures in Fe(III) oxyhydroxides may thus be used to explore for paleo-hydrothermal systems in ancient island-arc settings. In particular, the anomalous arsenic concentrations in Tutum Bay Fe(III) oxyhydroxides would be of great interest if found during a geochemical exploration program. The Tutum Bay vents are connected to the much larger hydrothermal system present beneath Ambitle Island (Pichler et al., 1999b) and they are only a few kilometers distant from the Kabang gold prospect (Licence et al., 1987).

7. Summary and conclusions

Ambitle Island is in several ways analogous to a seamount with the exception that it is not completely submerged, although its greater part is under water and during its history it may have been longer a seamount than an island. The hydrothermal system here clearly demonstrates the separation into sulfide mineralization, deposited at depth (Licence et al., 1987) and Fe(III) oxyhydroxide mineralization, deposited stratigraphically higher and at the margin of the hydrothermal system. Phase separation in the deep reservoir beneath Ambitle Island produces a low chlorinity, CO_2-rich hydrothermal fluid where sulfide is practically absent (< 0.01 mg/kg) (Pichler et al., 1999b). This fluid is highly reactive and Fe is leached form the host rock in the shallow sub-seafloor prior to discharge and Fe(III) oxyhydroxide precipitation commences upon mixing with ambient seawater.

With the exception of the unusually high arsenic values, the Tutum Bay Fe(III) oxyhydroxide deposits are in many respects similar to deposits found in much deeper water. Their hydrothermal origin is suggested by field observations and supported by chemical and mineralogical data. Precipitation Fe(III) oxyhydroxides from the hydrothermal fluid is due to mixing with ambient seawater. Mixing simultaneously increases the pH and Eh, and decreases temperature, all of which favor the precipitation of a Fe(III) oxyhydroxide. Based on measurements of $^{87}Sr/^{86}Sr$ ratios in Fe(III) oxyhydroxide, hydrothermal fluid and seawater, precipitation temperatures are estimated to be between approximately 60° and 90°C, in good agreement with previous studies of Fe(III) oxyhydroxide precipitation. Rapid precipitation and subsequent aging, in contact with seawater and/or a mixture of seawater and hydrothermal fluid (seawater $\gg$ hydrothermal fluid), is the suggested cause for the observed mineralogy. Rapid precipitation causes protoferrihydrite to be the main mineral phase in Tutum Bay Fe(III) oxyhydroxides. With increasing age and under oxidizing conditions nontronite, gypsum and various As-minerals are formed.

Rare earth element patterns of Fe(III) oxyhydroxides are closely controlled by the hydrothermal fluid and their incorporation happens without noticeable fractionation. The absolute concentration of REEs and selected trace elements (Rb, Tl, Sb and Cs) seems to be controlled by the extent of seawater mixing, as determined by the $^{87}Sr/^{86}Sr$ mixing model.

Arsenic concentrations in Tutum Bay Fe(III) oxyhydroxides are, by more than an order of magnitude, higher than those from other marine occurrences. The high concentrations are a direct result of the strong sorption ability of the high specific surface material, protoferrihydrite, at a pH of approximately 7 and at sufficient arsenic concentration in the hydrothermal fluid. Arsenic is successfully retained in the Fe(III) oxyhydroxide deposits because oxidizing conditions and high arsenic concentration allow for the formation of discrete arsenic minerals, such as claudetite, arsenic oxide and scorodite.

Acknowledgements

Most of this research was funded by an American Chemical Society, Petroleum Research Grant (No. 31585-AC8) and a Natural Sciences and Engineering Research Council of Canada operating grant to Jan Veizer. Thomas Pichler acknowledges the support of two Geological Society of America, Student Research Grants (No. 5681-95 and 5904-96) and a McKinstry Scholarship (Society of Economic Geologists). Denis Rancourt, University of Ottawa, is

thanked for the Mössbauer analyses and Danielle Fortin, University of Ottawa, provided valuable comments on an earlier draft of this manuscript and helped with the TEM analysis. The comments of Peter Sedwick and an anonymous reviewer were greatly appreciated and helped to improve the quality of our manuscript. [MB]

References

Alt, J.C., 1988. Hydrothermal oxide and nontronite deposits on seamounts in the Eastern Pacific. Marine Geology 81, 227–239.

Alt, J.C., 1993. Low-temperature alteration of basalts from the Hawaiian Arch, Leg 136. Proceedings of the Ocean Drilling Program, Scientific Results, Vol. 136.

Andrews, A.J., 1980. Saponite and celadonite in layer 2 basalts, DSDP Leg 37. Contributions to Mineralogy and Petrology 73, 323–340.

Berger, B.R., Silberman, M.L., 1985. Relationships of trace element patterns to geology in hot-spring type precious metal deposits. In: Berger, B.R., Bethke, P.M. (Eds.), Geology and Geochemistry of Epithermal Systems. Economic Geology, pp. 232–248.

Binns, R.A. et al., 1993. Hydrothermal oxide and gold-rich sulfate deposits of Franklin seamount, western Woodlark Basin, Papua New Guinea. Economic Geology 88 (8), 2122–2153.

Bischoff, J.L., 1969. Red Sea geothermal brine deposits: their mineralogy, chemistry, and genesis. In: Degens, E.T., Ross, D.A. (Eds.), Hot Brines and Recent Heavy Metal Deposits in the Red Sea. Springer Verlag, New York, pp. 368–401.

Bonatti, E., Kraemer, T., Rydell, H., 1972. Classification and genesis of iron–manganese deposits. In: Horn, D.R. (Ed.), Ferro-Manganese Deposits on the Ocean Floor. Harriman, Arden House and Lamont-Doherty Geological Observatory, New York, pp. 149–166.

Bowell, R.J., 1994. Sorption of arsenic by iron oxides and oxyhydroxides in soils. Applied Geochemistry 9, 279–286.

Boyle, R.W., Jonasson, I.R., 1973. The geochemistry of arsenic and its use as an indicator element in geochemical prospecting. Journal of Geochemical Exploration 2, 251–296.

Bruhn, F. et al., 1995. Diagenetic history of sedimentary carbonates: constraints from combined cathodoluminescence and trace element analyses by micro-PIXE. Nuclear Instruments and Methods 104, 409–414.

Carpenter, J.H., Grant, V.E., 1967. Concentration and state of cerium in coastal waters. Journal of Marine Research 25, 228–238.

Chao, T.T., Theobald, J.P.K., 1976. The significance of secondary iron and manganese oxides in geochemical exploration. Economic Geology 71, 1560–1569.

Chukhrov, F.V., Groshkov, A.I., Zirijagin, B.B., Yermilova, L.P., Balashova, V.V., 1973. Ferrihydrite. International Geology Review 16 (10), 1131–1143.

Cremer, M.D., 1995. Geochemistry of hydrothermal deposits from the summit region of Loihi Seamount, Hawaii. MS Thesis, University of Hawaii, Honolulu, 71 pp.

Davis, J.A., Kent, D.B., 1991. Surface complexation modeling in aqueous geochemistry. In: Hochella, M.F., White, A.F. (Eds.), Mineral–Water Interface Geochemistry. Reviews in Mineralogy. Mineralogical Society of America, Washington, pp. 177–260.

Deer, W.A., Howie, R.A., Zussmann, J., 1992. An Introduction to the Rock-Forming Minerals. Longman Scientific and Technical, Essex, 696 pp.

Drever, J.I., 1988. The Geochemistry of Natural Waters. Prentice-Hall, Englewood Cliffs, 392 pp.

Dzombak, D.A., Morel, F.M.M., 1990. Surface Complexation Modeling: Hydrous Ferric Oxide. Wiley-Interscience, New York.

Edmond, J.M. et al., 1979. On the formation of metal-rich deposits at ridge crests. Earth Planetary Science Letters 46, 19–30.

Faure, G., 1986. Principles of Isotope Geochemistry. Wiley, New York, 589 pp.

Faure, G., 1991. Principles and Applications of Inorganic Geochemistry. Macmillan, New York, 626 pp.

Fleet, A.J., 1984. Aqueous and sedimentary geochemistry of the rare earth elements. In: Henderson, P. (Ed.), Rare Earth Element Geochemistry. Developments in Geochemistry, Elsevier, pp. 343–373.

Fortin, D., Leppard, G.G., Tessier, A., 1993. Characteristics of lacustine diagenetic iron oxyhydroxides. Geochimica et Cosmochimica Acta 57, 4391–4404.

Gallahan, W.E., Duncan, R.A., 1994. Spatial and temporal variability in crystallisation of celadonites within the Troodos Ophiolite, Cyprus: implications for low-temperature alteration of the oceanic crust. Journal of Geophysical Research 99, 3147–3161.

Giessen, A.A., 1966. The structure of iron (III) oxide hydrate gel. Journal of Inorganic Nuclear Chemistry 28 (10).

Goldberg, E.D., 1961. Chemistry in the oceans. In: Sears, M. (Ed.), Oceanography. American Association of Advanced Scientific Publications, pp. 583–597.

Haskin, L.A., Haskin, M.A., Frey, F.A., Wildman, T.R., 1968. Relative and absolute terrestrial abundance of the rare earths. In: Ahrens, L.H. (Ed.), Origin and Distribution of the Elements. Pergamon, Oxford, pp. 889–911.

Hein, J.R., Yeh, H.-W., Gunn, S.H., Gibbs, A.E., Wang, C.-H., 1994. Composition and origin of hydrothermal ironstones from central Pacific seamounts. Geochimica et Cosmochimica Acta 58, 179–189.

Hekinian, R. et al., 1993. Hydrothermal Fe and Si oxyhydroxide deposits from South Pacific intraplate volcanoes and East Pacific Rise axial and off-axial regions. Economic Geology 88 (8), 2099–2121.

Koeppenkastrop, D., De Carlo, E.H., 1992. Sorption of rare-earth elements from seawater onto synthetic mineral particles: an experimental approach. Chemical Geology 95, 251–263.

Koeppenkastrop, D., De Carlo, E.H., Roth, M., 1991. A method to investigate the interaction of rare earth elements in aqueous

solution with metal oxides. Journal of Radioanalysis and Nuclear Chemistry 152, 337–346.

Leblanc, M. et al., 1996. Accumulation of arsenic from acid mine waters by ferruginous bacterial accretions (stromatolites). Applied Geochemistry 11, 541–554.

Lee, J.H., Bryne, R.H., 1993. Complexation of trivalent rare earth elements (Ce, Eu, Gd, Tb, Yb) by carbonate ions. Geochimica et Cosmochimica Acta 57, 295–302.

Licence, P.S., Terrill, J.E., Fergusson, L.J., 1987. Epithermal gold mineralization, Ambitle Island, Papua New Guinea, Pacific Rim Congress 87. Australasian Institute of Mining and Metallurgy, Gold Coast, Queensland, pp. 273–278.

Malahoff, A., McMurtry, G.M., Wiltshire, J.C., Yeh, H.-W., 1982. Geology and chemistry of hydrothermal deposits from active submarine volcano Loihi, Hawaii. Nature 298 (5871), 234–239.

Manning, B.A., Goldberg, S., 1997. Adsorption and stability of arsenic(III) at the clay mineral–water interface. Environmental Science and Technology 31, 2005–2011.

Maxwell, J.A., Teesdale, W.J., Campbell, J.L., 1995. The Guelph PIXE software package II. Nuclear Instruments and Methods in Physics Research B 95, 407–421.

McMurtry, G.M., Yeh, H.W., 1981. Hydrothermal clay mineral formation of East Pacific Rise and Bauer Basin sediments. Geology 32, 189–205.

Michard, A. et al., 1993. Submarine thermal springs associated with young volcanoes: the Teahitia vents, Society Islands, Pacific Ocean. Geochimica et Cosmochimica Acta 57, 4977–4986.

Millero, F.J., Sotolongo, S., Izaguirre, M., 1987. The oxidation kinetics of Fe(II) in seawater. Geochimica et Cosmochimica Acta 51, 793–801.

Müller, D., Groves, D.I., 1993. Direct and indirect associations between potassic igneous rocks, shoshonites and gold–copper deposits. Ore Geology Reviews 8, 383–406.

Murnane, R., Clague, D.A., 1983. Nontronite from a low-temperature hydrothermal system on the Juan de Fuca Ridge. Earth Planetary Science Letters 65, 343–352.

Murray, J.W., 1979. Iron oxides. In: Burns, R.G., (Ed.), Marine Minerals. Mineralogical Society of America, Washington, pp. 47–98.

Olivarez, A.M., Owen, R.M., 1989. REE/Fe variations in hydrothermal sediments: implications for the REE content of seawater. Geochimica et Cosmochimica Acta 53, 757–762.

Parker, R.J., Nicholson, K., 1990. Arsenic in geothermal sinters: determineation and implications for mineral exploration. In: Harvey, C.C., Browne, P.R.L., Freestone, D.H., Scott, G.L. (Eds.), 12th NZ Geothermal Workshop. Auckland University, Auckland, pp. 35–39.

Pichler, T., 1998. Shallow-water hydrothermal activity in a coral-reef ecosystem, Ambitle Island, Papua New Guinea. PhD Thesis, Univerity of Ottawa, Ottawa, 206 pp.

Pichler, T., Hutchinson, R.W., 1993. Gold mineralization in the marine environment: a possible marine mineral exploration and mining target. 24th Underwater Mining Institute, Estes Park, Colorado.

Pichler, T., Dix, G.R., 1996. Hydrothermal venting within a coral reef ecosystem, Ambitle Island, Papua New Guinea. Geology 20 (5), 435–438.

Pichler, T., Veizer, J., Hall, G.E.M., 1999a. Natural input of arsenic into a coral-reef ecosystem by hydrothermal fluids and its removal by Fe(III) oxyhydroxides. Environmental Science and Technology 33 (9), 1373–1378.

Pichler, T., Veizer, J., Hall, G.E.M., 1999b. The chemical composition of shallow-water hydrothermal fluids in Tutum Bay, Ambitle Island, Papua New Guinea and their effect on ambient seawater. Marine Chemistry 64 (3), 229–252.

Pierce, M.L., Moore, C.B., 1980. Adsorption of arsenite on amorphous iron hydroxide from dilute aqueous solution. Environmental Science and Technology 14, 214–216.

Puteanus, D., Glasby, G.P., Stoffers, P., Kunzendorf, H., 1991. Hydrothermal iron-rich deposits from the Teahitia–Mehitia and Macdonald hot spot areas, Southwest Pacific. Marine Geology 98, 389–409.

Rad, v.U., Frenzel, G., Muehe, R., 1990. Origin and alteration of submarine volcanoclastic rocks from the Lau and North Fiji basins. Geolgisches Jahrbuch, D 92, 341–393.

Rona, P.A., 1984. Hydrothermal mineralization at seafloor spreading centers. Earth-Science Reviews 20, 1–104.

Schwertmann, U., 1966. Die bildung von Eisenoxidmineralien. Fortschritte der Mineralogie 46, 274–285.

Schwertmann, U., 1970. Der Einfluss einfacher organischer Anionen auf die Bildung von Goethit und Haematit aus amorphen Fe(III) hydroxid. Geoderma 3, 207–214.

Schwertmann, U., Fischer, R.W., 1973. Natural 'amorphous' ferric hydroxide. Geoderma 10, 237–247.

Sedwick, P.N., McMurtry, G.M., 1987. Transition metals in Loihi Seamount hydrothermal solutions. EOS 68, 1554.

Sedwick, P.N., McMurtry, G.M., Macdougall, J.D., 1992. Chemistry of hydrothermal solutions from Pele's Vents, Loihi Seamount, Hawaii. Geochimica et Cosmochimica Acta 56, 3643–3667.

Seyfried, W.E. Jr., Bischoff, J.L., 1977. Hydrothermal transport of heavy metals by seawater: the role of seawater/basalt ratio. Earth Planetary Science Letters 34, 71–77.

Silberman, M.L., Berger, B.R., 1985. Relationships of trace element patterns to alteration and morphology in epithermal precious metal deposits. In: Berger, B.R., Bethke, P.M. (Eds.), Geology and Geochemistry of Epithermal Systems. Economic Geology, pp. 203–232.

Sillitoe, R.H., 1988. Environments, styles and origins of gold deposits in western pacific island arcs.

Stakes, D.S., Scheidegger, K.F., 1981. Temporal variations in secondary minerals from Nazca Plate basalts. In: Kulm, L.D. (Ed.), Nazca Plate: Crustal Formation and Andean Convergence. Geological Society of America, pp. 109–130.

Stoffers, P., Singer, A., McMurtry, G.M., Arquit, A., Yeh, H.-W., 1990. Geochemistry of a hydrothermal nontronite deposit from the Lau Basin, southwest Pacific. Geologisches Jahrbuch, D 92, 615–628.

Stoffers, P. et al., 1993. Comparative mineralogy and geochemistry of hydrothermal iron-rich crusts from the Pitcairn, Teahitia–Meahitia, and Macdonald hot spot areas of the S.W. Pacific. Marine Georesources and Geotechnology 11, 45–86.

Stumm, W., Morgan, J.J., 1996. Aquatic Chemistry. Wiley-Interscience, New York, 1022 pp.

Towe, K.M., Bradley, W.F., 1967. Mineralogical constitution of colloidal 'hydrous ferric oxides'. Journal of Colloid and Interface Science 24 (3), 384–392.

Varnavas, S.P., Cronan, D.S., 1991. Hydrothermal metallogenic processes off the islands of Nisiros and Kos in the Hellenic Volcanic Arc. Marine Geology 99, 109–133.

Wallace, D.A. et al., 1983. Cainozoic volcanism of the Tabar, Lihir, Tanga, and Feni islands, Papua New Guinea: geology, whole-rock analyses, and rock-forming mineral compositions. 243, Bureau of Mineral Resources Geology and Geophysics, Sydney.

Weisgerber, G., 1982. Towards a history of copper mining in Archaeology. In: Muhly, J.D., Maddin, R., Karageorghis, V. (Eds.), Early Metallurgy in Cyprus. Pierides Foundation, Nicosia, Cyprus, pp. 382.